ASME Journal of Manufacturing Science and Engineering
Online journal at:
https://asmedigitalcollection.asme.org/manufacturingscience

Shuichi Amano[1]
Nissei Co., Ltd.,
2022 Tomihamamachi Torisawa,
Otsuki, Yamanashi 409-0502, Japan
e-mails: s_amano@nisseiweb.co.jp;
s_amano_dt26@nisseiweb.co.jp

Toshinaka Shinbutsu
Nissei Co., Ltd.,
2022 Tomihamamachi Torisawa,
Otsuki, Yamanashi 409-0502, Japan
e-mail: t_shinbutsu@icloud.com

Yuki Okimoto
Nissei Co., Ltd.,
2022 Tomihamamachi Torisawa,
Otsuki, Yamanashi 409-0502, Japan
e-mail: y_okimoto@nisseiweb.co.jp

Teruie Takemasu
Professor
Faculty of Future Industry,
Happy Science University,
4427-1 Hitotsumatsu Hei, Chosei-mura,
Chosei-gun, Chiba 299-4325, Japan
e-mail: t_tkms@happy-science.university

Jyo Shimura
Professor
Department of Mechanical Systems Engineering,
Takushoku University,
815-1 Tatemachi, Hachioji,
Tokyo 193-0985, Japan
e-mail: jshimura@ms.takushoku-u.ac.jp

Osamu Hasegawa
Mechanical Systems Engineering Program,
Tokyo Metropolitan College of Industrial Technology,
1-10-40 Higashi-oi, Shinagawa,
Tokyo 140-0011, Japan
e-mail: hasegawa@metro-cit.ac.jp

Toshihiko Kuwabara
Professor
Division of Advanced Mechanical Systems Engineering,
Institute of Engineering, Tokyo University of Agricultural and Technology,
2-24-16 Naka-cho, Koganei-shi,
Tokyo 184-8588, Japan
e-mail: kuwabara@cc.tuat.ac.jp

Rolling Formability Optimization of Locking Bolt Based on a Double-Thread Structure Composed of Coaxial Single and Multiple Threads

In previous studies, we developed innovative anti-loosening bolts and nuts with a double-thread structure (denoted DTB-IIC) composed of coaxial single and multiple coarse threads. It was also experimentally proven that the DTB-IIC has high anti-loosening performance. In this study, we analytically and experimentally investigated the effects of multiple thread groove depths and rolling methods on the thread rolling formability of DTB-IIC fasteners. The bottom rise rate, which is the ratio of the bottom rise amount of the multi-thread groove to the reference thread height, was set in three ways of 50%, 60%, and 70%. As the bottom rise rate increased, peeling on the thread surface was suppressed and the high temperatures produced by thread rolling decreased significantly, but the loosening resistance against vibration clearly decreased. We compared three typical mass production processes for bolts: the round die method, the flat die method, and the planetary method, with the bottom rise rate set at 50%. It was found that the flat die method had the best rolling formability in terms of screw-thread shape and surface quality. A finite element simulation consistently reproduced the deformation process of the complex DTB-IIC thread and revealed that the material shear flow due to over-rolling led to the occurrence of surface peeling.
[DOI: 10.1115/1.4067013]

Keywords: anti-loosening bolt, double-thread mechanism, thread rolling, bottom rise rate, rolling method, rolling formability, strength tests, Junker vibration loosening test, design for manufacturing, modeling and simulation, production systems optimization, welding and joining

1 Introduction

Screw fasteners are clearly one of the most vital and useful machine elements due to their ease of installation and removal.

[1]Corresponding author.
Manuscript received May 28, 2024; final manuscript received September 20, 2024; published online November 18, 2024. Assoc. Editor: Naohiko Sugita.

They have been used for a very long time in the Western world, and currently are spread almost worldwide. In particular, bolt fasteners smaller than M24 are manufactured in hundreds of billions annually around the world through established mass production processes using thread rolling. However, such small bolted joints have the problem of loosening due to the return rotation of the nut when dynamic external forces such as cyclic stress or impact force are applied during service [1]. This problem has not been completely solved, and fatal accidents caused by such failures are still being reported around the world [2]. Therefore, many researchers have investigated the cause of loosening of bolted joints [3–6] and considered many different countermeasures [7–10]. Most commercially available anti-loosening screw-parts exhibit macro-slip on the nut-bearing surface when subjected to a severe transverse vibration load and cannot completely suppress rotational loosening because most of them only enhance the frictional force between the bolt and nut or between the nut and the bearing surface [5,11–14]. In comparison, it has been proven that double-thread bolt (DTB) fasteners, which have two types of coaxial screw thread with different lead angles, have excellent anti-loosening properties [15–17]. For such fasteners, a higher lead nut is first installed, and then a lower lead nut is added to form a double-nut structure. The anti-loosening mechanism for DTBs is enhanced by mechanical locking based on the interference effect of two kinds of nut with different loosening speeds.

Various screw-thread structures are possible for DTBs, but in previous studies [18–20], we have devised the DTB-II with an innovative double-thread mechanism composed of a single coarse thread and multiple coarse threads, and investigated the optimization of its structure, anti-loosening performance, and mass production potential. The results showed that the innovative anti-loosening bolts and nuts with a double-thread structure (DTB-IIC) shown in Fig. 1(*a*) has an overall superior structure from the viewpoints of rolling formability, static and dynamic tensile strength, and vibration loosening resistance [20,21]. The DTB-IIC has a thread structure in which the number of multiple thread grooves is set to three, then one thread groove is removed, the remaining two thread grooves are aligned at a 1.5-pitch interval, and the depth of these grooves is reduced by up to 50% of the thread height. Nut fastening and torque management for DTB-II can be performed very easily because the inner multi-thread nut, mounted first as shown in Fig. 1(*c*), is also rotated when the outer single-thread nut is tightened, solving most of the problems encountered with the conventional DTB-I [16]. Mass production of the DTB-IIC is carried out in the same way as a normal single-thread bolt (STB) using dedicated dies with a complicated groove profile on the processing surface, as shown in Fig. 2, which has almost the same contour as the thread profile for a DTB-IIC bolt at each corresponding angular position, as shown in Fig. 1(*b*). Previously, the machining of the special grooves in DTB-IIC dies was carried out by electrical discharge machining, which was very time-consuming and costly, making it impractical. Thus, in our previous study [21], we successfully established a high-precision grinding system to manufacture a dedicated die for DTB-IICs with high speed and high efficiency. As a result, the production cost and processing time were reduced drastically, and by optimizing the die groove shape (specifically, the length and depth of the parallelogram groove shown in Fig. 2(*b*)), the mating state between a rolled DTB-IIC bolt and the inner multi-thread nut could be adjusted appropriately.

However, some issues still remained, such as the occurrence of material peeling on the rolled thread surface and the high temperature produced in the workpiece by thread rolling compared to the temperature induced by STB processing. To further improve the practicality of this technology in the future, it is necessary to establish a mass production process that improves rolling formability to the same level as that of STBs. In the present study, to solve these problems, we first focused on the bottom rise rate β of the multi-thread groove, and made some modified DTB-IICs with β larger than 50% of the value used in a previous study [20] and conducted finite element method (FEM) simulations and experiments of thread rolling. The first purpose of this study was to quantitatively evaluate the effects of β on rolling formability, strength, and vibration loosening resistance. Next, we evaluated three types of mass production processes for bolt threads: the round die method, the flat die method, and the planetary method. Until now, thread rolling experiments in this research have only been conducted using the round die method, because it is easy to change the rolling conditions. But, at actual production sites, most high-demand M24 or smaller bolts are thread-rolled using the flat die method or the planetary method due to higher productivity. Hence, using the above-mentioned die grinding system, we developed dedicated rolling dies that are compatible with the flat die and planetary methods, and carried out rolling experiments and simulations using them. The second purpose of this study was to comparatively evaluate the effects of different thread rolling methods on thread formability.

2 Method

2.1 Thread Structure of Modified DTB-IIC. For the reason given above, this study used a conventional DTB-IIC and its modified version as the research targets. Figure 1(*a*) shows the fundamental thread structure of the DTB-IIC, and Fig. 1(*b*) shows the cross-sectional shape of the threads at each representative angular position from 0 deg to 180 deg along the half circumference of the bolt. Here, the bottom rise rate β for the multi-thread groove is defined as the value obtained by dividing the amount of bottom rise α by the reference thread height h, expressed as a percentage. In this study, we investigated the conventional DTB-IIC with β set to 50%, which is the effective diameter position, and two modified DTB-IICs with β set to 60% and 70%. Each specimen is denoted as DTB-IIC50, DTB-IIC60, and DTB-IIC70, respectively. The threads of these DTB-IICs were rolled using dedicated dies in which the depth of the trapezoidal groove was adjusted according to

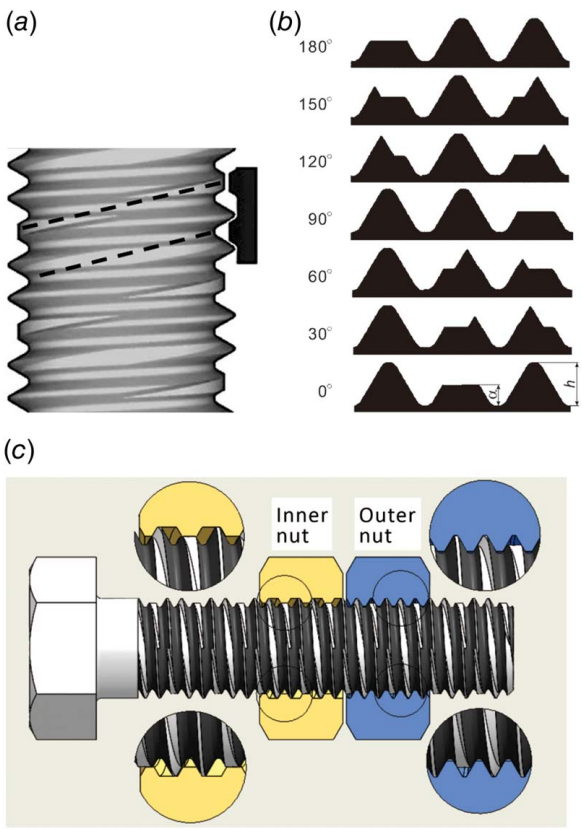

Fig. 1 Thread structure of DTB-IIC: (*a*) thread structure, (*b*) cross-sectional profiles, and (c) mating details with two types of nuts

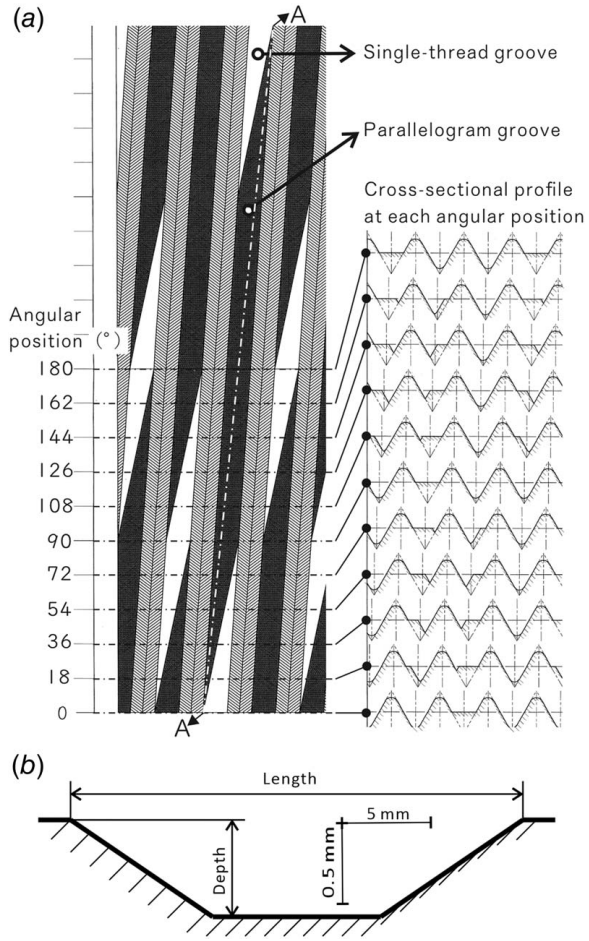

Fig. 2 Appearance of dedicated rolling die for DTB-IIC: (*a*) cross-sectional profile at each angular position and (*b*) A–A cross-sectional profile of the parallelogram groove

β, as shown in Fig. 2(*a*). Figure 3 shows the changes in the circumferential direction of the thread cross-sectional area ratio, ξ, for each DTB-IIC type, which was calculated by dividing the thread cross-sectional area for three pitches at each angular position of the DTB-IIC by that for the normal STB. As β increases, the minimum value of ξ gradually approaches 100%, and its distribution becomes linear. As a result, the thread shape for DTB-IIC70 in particular is almost the same as that for a normal STB, which is expected to improve rolling formability.

2.2 Thread Rolling Experiments. For a comparative evaluation, thread rolling experiments were conducted on DTB-IICs with a nominal size of M12 × 1.75 as in a previous study [20]. The bolt materials were AISI 1045 raw material and AISI 4135 heat-treated material. For DTB-IIC50, we conducted thread rolling experiments using the three processes mentioned above, but for DTB-IIC60 and DTB-IIC70, we used only the round die method, which allows us to flexibly change conditions such as the amount of die radial feed and the number of times the workpiece is rolled. Round die rolling was carried out by attaching dedicated round dies to a manual hydraulic rolling machine with a two-roller die plunge feed (FA-16U, Nissei Co., Ltd.) with a die rotational speed of 62 min^{-1} and a rolling time of 3 s including 1 s of dwell (approximately 30 rotations of the workpiece). Flat die rolling was performed in an inverter-type thread rolling machine (HR-FM2, Higashida Machinery Co., Ltd.), in which dedicated dies were attached to both the fixed and movable sides, and a one-side sliding method was used. The processing time was approximately

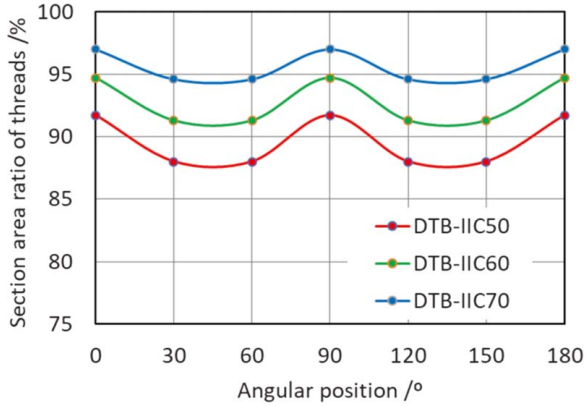

Fig. 3 Comparison of changes in sectional area ratio of screw threads at each angular position

0.45 s with seven rotations for workpiece forming and two rotations for dwelling. For the planetary method, a rotary rolling machine (SSR-50D, Sakamura Machine Co., Ltd.) was used, and a dedicated segment die on the stationary side was installed with appropriate eccentricity relative to the dedicated round die on the drive side. The processing time was approximately 0.33 s with nine rotations of the workpiece. The initial diameter of the bolt material and the amount of die radial feed were adjusted as appropriate based on the thread forming condition and inspection using a gauge nut.

2.3 Thread Rolling Simulation of DTB-IICs. To analyze the rolling formability of DTB-IICs, thread rolling simulations were performed using simplified 3D FEM models. The commercial code Simufact.forming ver.15 was adopted. Figure 4(*a*) shows the initial FEM mesh for the cylindrical workpiece. The height of the workpiece was restricted to an approximately 6-pitch length of the STB to reduce the calculation time, and the initial diameter was set to 10.8 mm due to the volume constancy condition. A semitransparent refinement box (RB) was placed in the region from an inner diameter of 8 mm to an outer diameter of 14 mm; this region was divided by fine hexahedral elements with a reference size of 0.4 mm. The mesh-rezoning procedures were conducted about 20 times during a whole thread rolling process. The material properties were assumed as the stress–strain relations corresponding to AISI 1045 raw material expressed in the form of power law by

$$\bar{\sigma} = 900\bar{\varepsilon}^{0.17} \tag{1}$$

where $\bar{\sigma}$ (MPa) is the equivalent stress and $\bar{\varepsilon}$ is the equivalent strain.

Figures 4(*b*) and 4(*c*) show the flat die and planetary FEM simulation models, respectively, in which the workpiece is an elasto-plastic material and the rolling dies are rigid bodies. The round die and flat die FEM models are basically the same, but performing a simulation using round dies under the same rolling conditions as the experiment would require too much calculation time (approximately 3 months), so it was replaced with the flat die model. During processing using flat dies in Fig. 4(*b*), the two dedicated dies were placed on both sides of the workpiece, each was moved synchronously in opposite directions (see arrows in the figure) and simultaneously pushed into the workpiece at the same constant speed by a specific amount of $\delta_{\max}$, dwelled, and then released. The workpiece was subjected to seven rotations for forming and two rotations for dwelling, as in the fabrication experiment. In the actual planetary rolling process, the segment die was fixed, only the round die was rotated, and the material was moved planetarily around its outer circumference to cut the threads. However, with the same approach, the RB cannot be placed around the workpiece because its spatial position is fixed in the simulation. To solve this

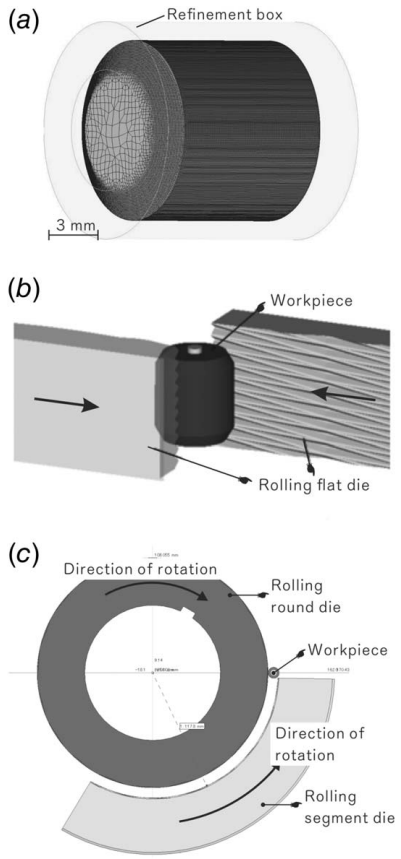

Fig. 4 FEM simulation models: (*a*) FEM mesh of the workpiece, (*b*) flat die rolling model, and (*c*) rotary planetary rolling model

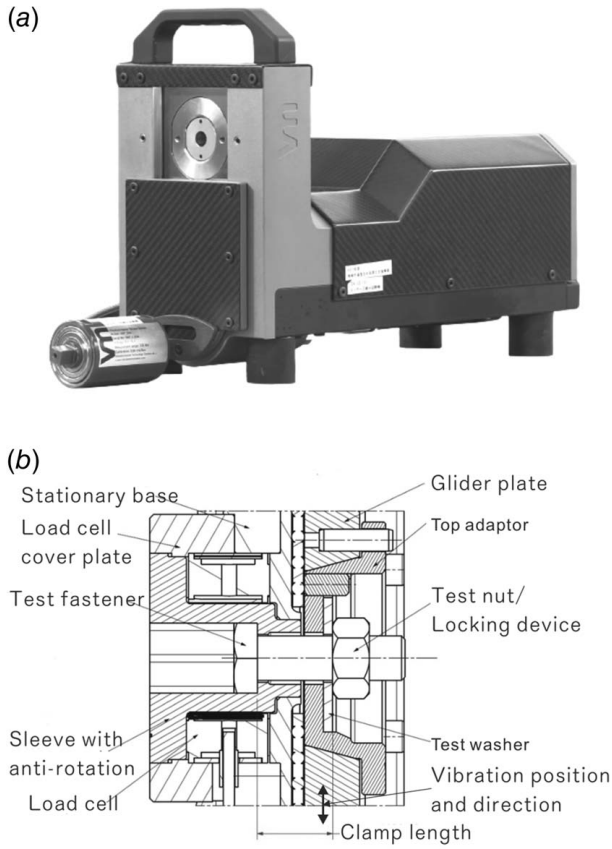

Fig. 5 Vibration loosening test apparatus: (*a*) Junker fastener test bench and (*b*) cross-sectional schematic diagram

problem, as shown in Fig. 4(*c*), the center of curvature of the processing surface of the segment die was placed eccentrically by a specified amount with respect to the rotation center of the round die, and thread rolling was performed by rotating both dies synchronously in the direction of the arrows. In either rolling method, the dedicated groove shown in Fig. 2 was precisely provided on the processing surface of all dies, and the workpiece was only allowed to rotate around its central axis and move in the die thrust direction. Coulomb's friction law was assumed in the contact area between the die and the workpiece, and the coefficient of friction was set to 0.2. Note that rolling simulations for DTB-IIC60 and DTB-IIC70 were conducted using the flat die method, which enabled us to reduce the calculation time significantly and to provide stable solutions compared to the round die method. Due to the volume constancy condition, δ_{max} was set as 0.64 mm for DTB-IIC50, 0.67 mm for DTB-IIC60, and 0.70 mm for DTB-IIC70.

2.4 Tensile Strength and Vibration Loosening Tests. Tensile strength tests and vibration loosening tests were conducted to compare the strength and loosening resistance of the three types of M12 DTB-IIC with different β values rolled using round dies. The bolt material was a chrome-molybdenum steel bar meeting specification AISI 4135 with a strength rank of grade 8 in SAE J429.

For the tensile tests, we used a universal tensile testing machine (AG-25TB, Shimadzu Corp.) equipped with a special rig with a self-aligning function in the axial direction. The under-head full length of the bolt specimen was 110 mm and the length of the screw portion was 58 mm. A test specimen mounted with a single screw nut 12 mm tall was placed in the rig and extended at a constant speed of 5 mm/min.

Vibration loosening tests based on ISO 16130 [22,23] were conducted using the Junker fastener test bench (J121, Vibrationmaster) shown in Fig. 5(*a*), which enables sequential observation of changes in the axial load of a bolted joint during testing. The bolt specimens were fully threaded with a length below the neck of 60 mm. Figure 5(*b*) illustrates the principle of Junker testing, in which a shear load due to transverse vibration of a glider plate is applied to the bolted joint, causing the nut to rotate backwards and loosen. This device allows for the optional specification of the initial axial preload F_M of the bolt, the transverse displacement amplitude A of the glider plate, the oscillation frequency f, and the total number of oscillations N (denoted as load cycles). F_M was set to 20 kN to approximate actual use, and A was set to 0.80 mm according to the self-loosening condition of a normal STB tightened using one nut as in the previous study [21]. f was set to the most severe condition of 12.5 Hz, and the test was terminated when N exceeded 2000 cycles (approximately 160 s) or when loosening of the bolted joint became apparent. The amount of F_M for the DTB-IIC joint was managed by adjusting the fastening torque of only the outer single-thread nut, and the back rotation of the inner multi-thread nut was omitted because the inner nut, which is mounted first, also rotates when the outer nut is tightened, as mentioned above. Molybdenum disulfide was used as a solid lubricant, and it was applied to the bolt threads before tightening the nut.

3 Results and Discussion

3.1 Effect of Bottom Rise Rate β on Rolling Formability. Figures 6(*a*), 6(*c*), and 6(*e*) compare the equivalent plastic strain distribution, $\bar{\varepsilon}$, in the final deformation state for the three types of DTB-IICs with different β values obtained by FEM simulation. Figures 6(*b*), 6(*d*), and 6(*f*) show the outer appearance of

experimentally thread-rolled samples made of the AISI 1045 raw material. Figures 7(*a*)–7(*c*) compare the screw-thread shapes for the three types of DTB-IICs obtained in the fabrication experiment. These figures are obtained by dividing the DTB-IIC into 12 sections at 15 deg intervals from 0 deg to 180 deg in the circumferential direction, measuring the thread profile at each angular position using SURFCOM 1800G (ACCRETECH), and connecting them. Figures 8(*a*)–8(*c*) compare the mating states for the three types of DTB-IICs and the corresponding inner multi-thread nut at 0 deg. Figures 9(*a*) and 9(*b*) show the filling state transitions for the material at the 0 deg and 45 deg positions of the die grooves at each die radial feed rate η [$\eta = (\delta/\delta_{\max}) \times 100\%$, where δ is the amount of die radial feed at each deformation stage and $\delta_{\max}$ is the final amount of die radial feed obtained from the FEM simulation.

Figure 6 shows that the final material piled-up state and the periodically changing thread profile for each DTB-IIC in the analysis (Figs. 6(*a*), 6(*c*), and 6(*e*)) agree well with the experiments (Figs. 6(*b*), 6(*d*), and 6(*f*)). Figures 7(*a*)–7(*c*) indicate that the target thread shapes for all cases are obtained for the entire external surface. It can also be clearly seen that as β increases, the DTB-IIC thread shape gradually approaches that of an STB. However, as shown in Fig. 8, the nominal contact area between the multi-thread groove and the inner multi-thread nut in the DTB-IIC70 is remarkably reduced compared to the DTB-IIC50, which may possibly have a negative effect on the vibration loosening resistance. Comparison of $\bar{\varepsilon}$ in Fig. 6 reveals no large difference among them, but since $\delta_{\max}$ increases somewhat as β increases, $\bar{\varepsilon}$ near the groove bottom of the single-thread groove becomes slightly larger: $\bar{\varepsilon} \cong 8.0$ for DTB-IIC50, 8.3 for DTB-IIC60, and 9.0 for DTB-IIC70. In contrast, $\bar{\varepsilon}$ near the bottom of the multi-thread groove becomes smaller as β increases: $\bar{\varepsilon} \cong 5.0$ for DTB-IIC50, 4.5 for DTB-IIC60, and 3.9 for DTB-IIC70. The reason for this is that in the DTB-IIC50, the shallower die grooves are almost completely filled at $\eta = 63\%$, as shown in Fig. 9(*a*), and the material at the

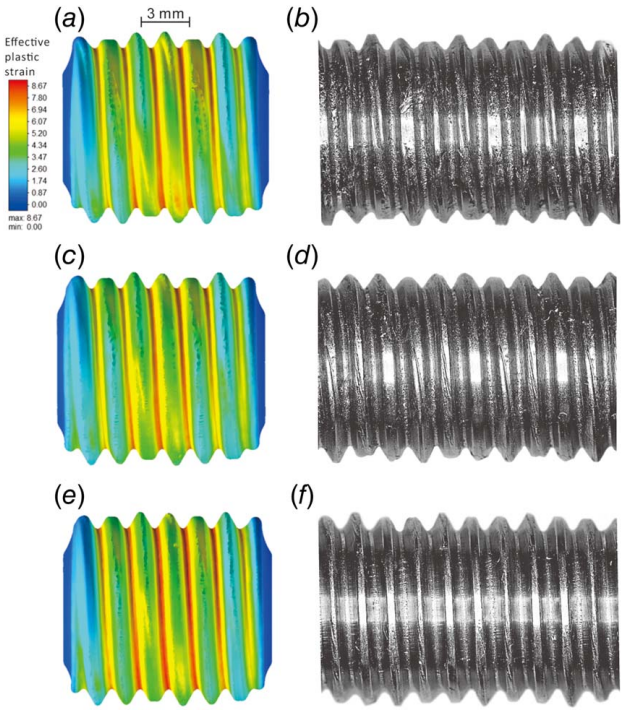

Fig. 6 Comparison of equivalent plastic strain distributions as calculated by FEM simulations and final products in experiments for three types of DTB-IICs: (*a*) DTB-IIC50 by FEM, (*b*) DTB-IIC50 in the experiment, (c) DTB-IIC60 by FEM, (*d*) DTB-IIC60 in the experiment, (e) DTB-IIC70 by FEM, and (*f*) DTB-IIC70 in the experiment

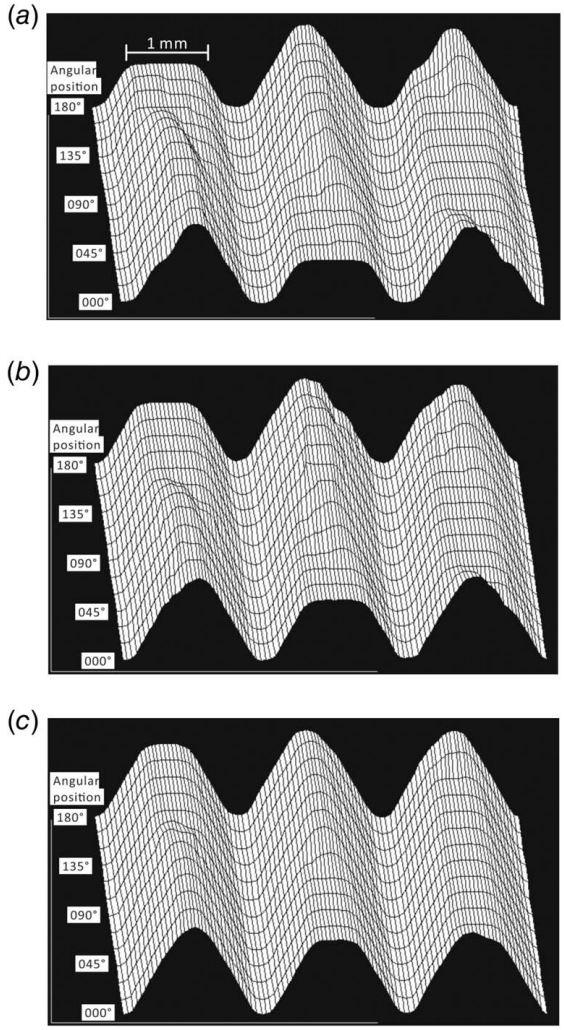

Fig. 7 Comparison of DTB-IIC rolled thread shapes in experiments: (*a*) DTB-IIC50, (*b*) DTB-IIC60, and (c) DTB-IIC70

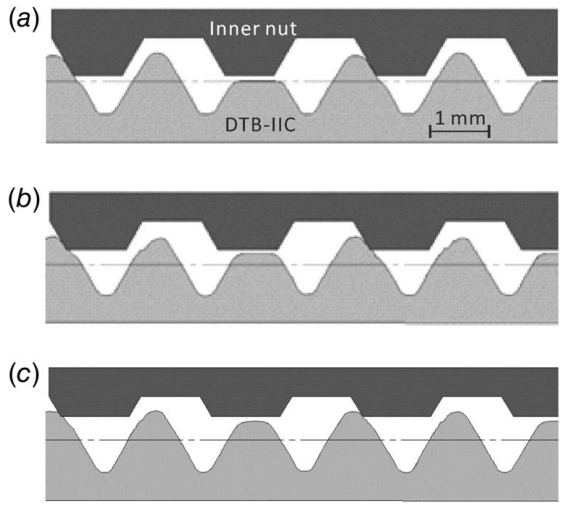

Fig. 8 Comparison of mating conditions between DTB-IICs and inner multi-thread nuts in experiments: (*a*) DTB-IIC50, (*b*) DTB-IIC60, and (c) DTB-IIC70

bottom of these grooves then becomes over-rolled. In contrast, for the DTB-IIC70, the completion of filling of the shallower die grooves is delayed at $\eta = 75\%$, as shown in Fig. 9(*b*), which reduces the degree of over-rolling. The material near completely filled grooves flows along the same single screw thread to the unfilled deeper grooves, and this material flow in the circumferential direction causes severe shear deformation, leading to material peeling at the surface. Accordingly, reducing the degree of over-rolling suppresses material peeling. In fact, comparison of the product thread surfaces in Fig. 6 shows that the DTB-IIC50 in Fig. 6(*b*) has a rough surface with small peeled regions in some places, while the DTB-II70 in Fig. 6(*f*) has a relatively smooth surface with slight peeling only at the groove bottom. In contrast, almost no peeling is observed for the heat-treated AISI 4135, even with DTB-IIC50. Table 1 compares the surface temperatures of various DTB-IICs immediately after thread rolling, measured using a non-contact thermometer (R-4601, Anritsu Meter Co., Ltd.). It can be seen that the temperature clearly decreases as β increases, and this tendency is particularly noticeable for the DTB-IIC70 compared to the DTB-IIC50. These results indicate that the rolling formability can be clearly improved by increasing β by 50% or more.

3.2 Effects of the Rolling Process Type on Rolling Formability. Figures 10(*a*) and 10(*b*) show the equivalent plastic strain distribution, $\bar{\varepsilon}$, and the material filling state in the final thread rolling stage for the DTB-IIC50 obtained by FEM simulation of the planetary method. Comparison of Figs. 10(*a*) and 6(*a*) shows that the flat die rolling process resulted in the desired thread with a sufficient height at all angular positions. In contrast, in the planetary process, two complete threads are formed at the 0 deg and 180 deg positions, but the thread height in the area surrounded by the dashed ellipse near 90 deg is insufficient (see Fig. 10(*b*)); the cause of this is currently unknown. In both processes, $\bar{\varepsilon}$ becomes a maximum at the bottom of the single thread, and its maximum value $\bar{\varepsilon}_{max}$ is approximately 9 in the flat die method and approximately 11 in the planetary method. This difference in $\bar{\varepsilon}_{max}$ depends on the number of workpiece rotations during forming: seven rotations for the flat die method and nine rotations for the planetary method.

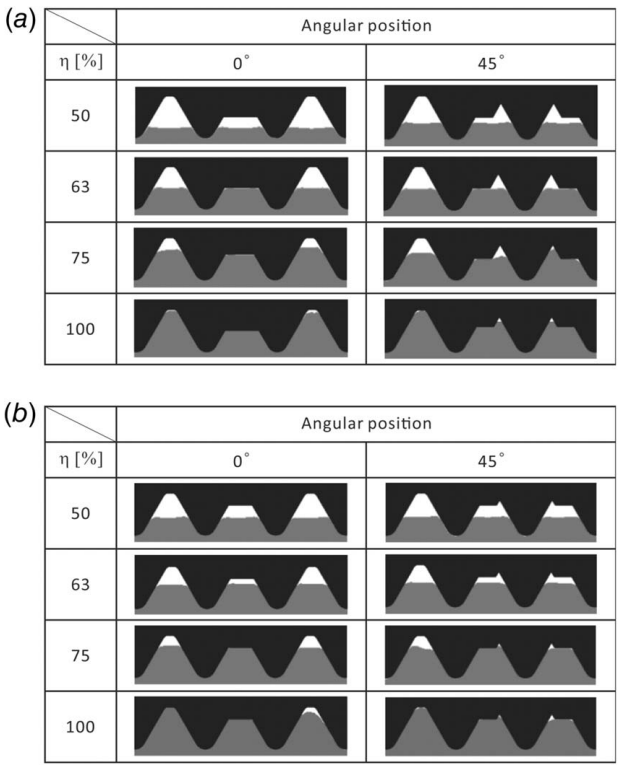

Fig. 9 Comparison of filling-up state in each die groove cross section, as calculated by FEM simulations: (*a*) DTB-IIC50 and (*b*) DTB-IIC70

Table 1 Bolt surface temperature after thread rolling

Bolt specimen	Surface temperature (°C)	
	AISI 1045	AISI 4315
DTB-IIC50	105	110
DTB-IIC60	82	100
DTB-IIC70	68	70

In the thread rolling experiments, because the initial diameter of the material and the die radial feed rate were adjusted appropriately, screw threads with sufficient height were obtained over the entire external surface in all rolling processes, as verified by inspection using a gauge nut. Thus, to evaluate the thread forming state in more detail, we compare the planar expanded 3D thread profiles for DTB-IIC50 obtained by each rolling process in Fig. 11. With the flat die method, as shown in Fig. 11(*a*), the desired threads were completely formed on the entire cross section, and the heights of the small threads around the ▼ marks at the 45 deg and 135 deg positions were also sufficient compared to those for the round die method shown in Fig. 7(*a*). However, this seems to be an issue with die machining accuracy, not with the rolling method. In contrast, with the planetary method shown in Fig. 11(*b*), the height of the thread in the elliptical region indicated by the dashed line is insufficient from 45 deg and 135 deg around the ★ mark on the left helical thread, as in the FEM simulation. However, the middle and right-side spiral threads were formed as intended. Figures 12(*a*) and 12(*b*) compare the product thread surfaces for the DTB-IIC50 made of AISI 1045 raw material rolled using the flat die and planetary methods. With both methods, there was almost no surface peeling of the material seen for the round die method shown in Fig. 6(*b*), and, in particular, the smoothest rolled surface was obtained with the flat die method. The main

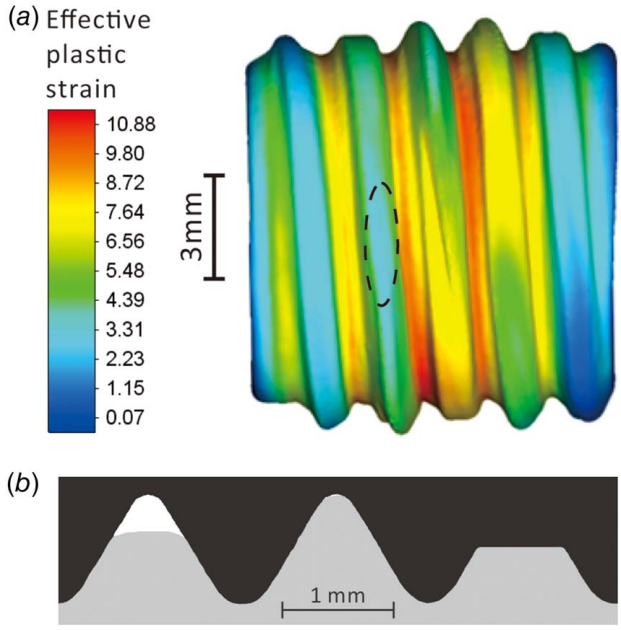

Fig. 10 Final deformation state for DTB-IIC50 rolled by the planetary method, as calculated by FEM simulations: (*a*) effective plastic strain distribution and (*b*) filling up state at 90 deg position

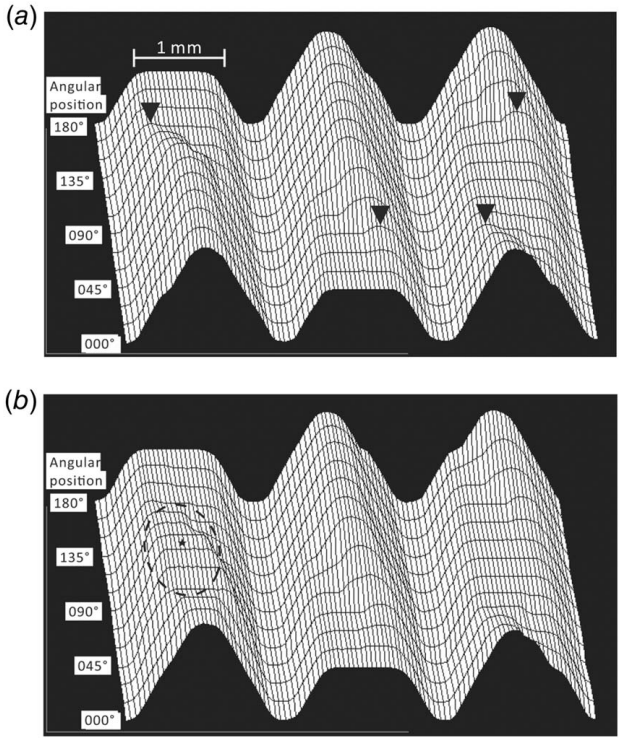

Fig. 11 Comparison of rolled thread shapes for DTB-IIC50s in experiments: (*a*) flat die method and (*b*) planetary method

reason for this is that, compared to the round die method, the total number of workpiece rotation during forming is less than one-third (9/30), and the contact area between the material and the die is considerably larger for the flat die method.

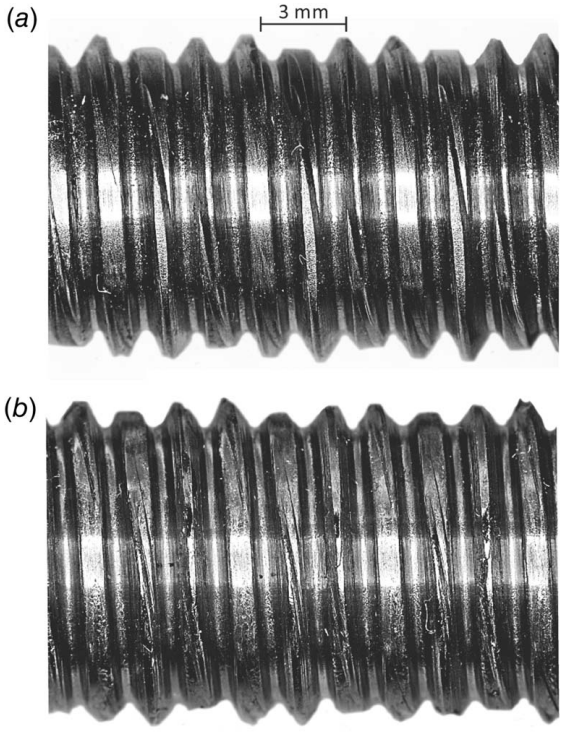

Fig. 12 Comparison of final products rolled by flat die and planetary methods in experiments: (*a*) flat die rolling and (*b*) planetary rolling

3.3 Tensile Strength of DTB-IIC Specimens. Figures 13(*a*)–13(*c*) compare load-stroke diagrams for the three types of DTB-IICs obtained from the static tensile tests. Each figure shows the results of three experiments. The failure mode for all bolt specimens was breaking of the base material without shear fracture of the screw threads. Comparison of these results shows that the tensile strength F_B for all DTB-IIC specimens exceeded the minimum tensile strength of 1040 N/mm^2 for SAE J429 strength grade 8 bolts. In addition, β had no effect on the tensile strength of the bolt specimens.

3.4 Vibration Loosening Tests. Figures 14(*a*)–14(*c*) show the variation in the residual rate of axial load κ with the number of load cycles N for the three types of DTB-IIC with different β values in the Junker vibration test. Each figure shows the results of three experiments. Here, the inner multi-thread nut of the DTB-IIC was fastened first by hand, and then the outer single-thread nut was fastened until the initial axial preload P_0 reached the specified value of 20 kN. According to the results reported in

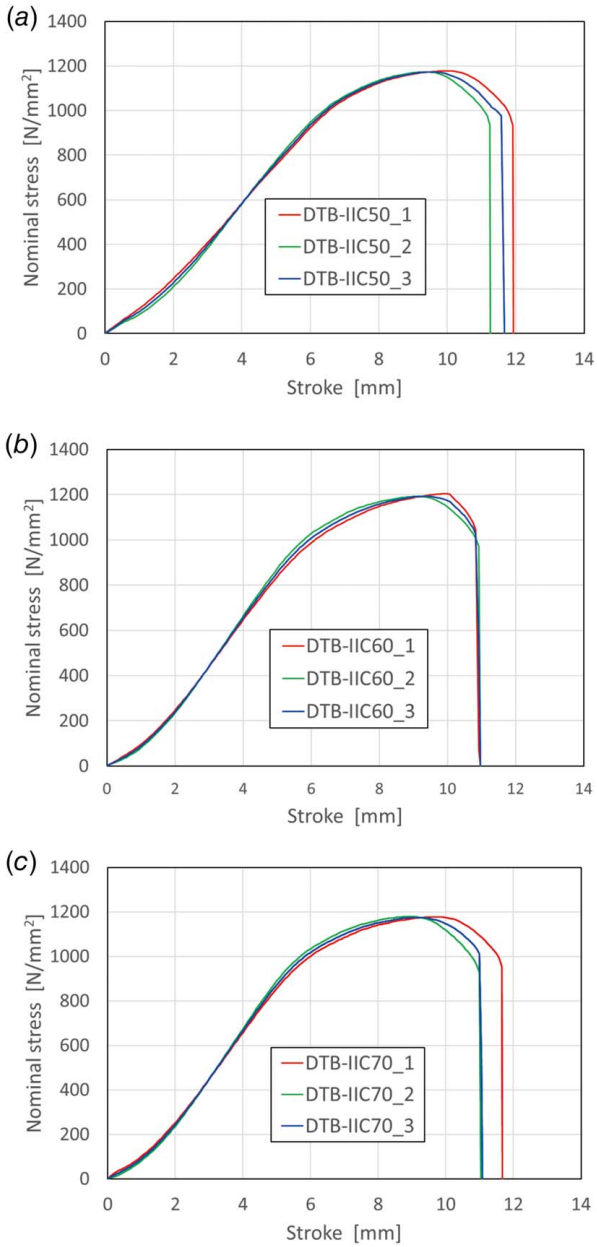

Fig. 13 Tensile strength test results: (*a*) DTB-IIC50, (*b*) DTB-IIC60, and (c) DTB-IIC70

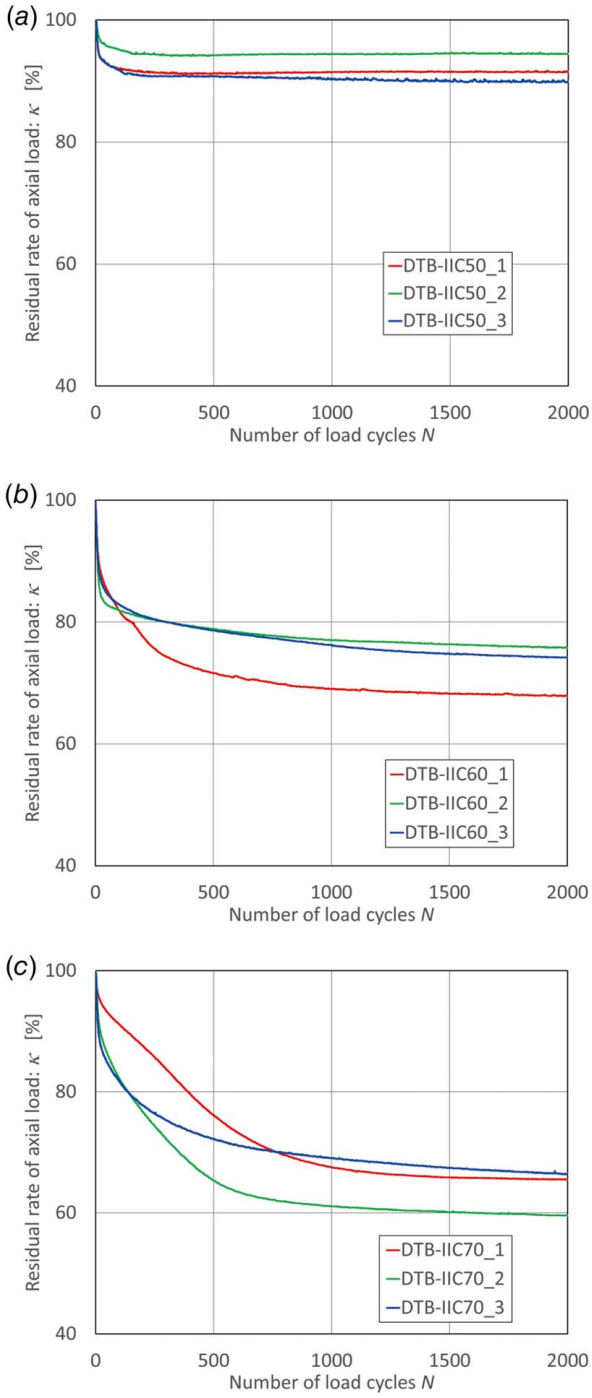

Fig. 14 Variation in residual rate of axial tension in Junker vibration loosening tests: (*a*) DTB-IIC50, (*b*) DTB-IIC60, and (*c*) DTB-IIC70

a previous paper [20], there was no difference in vibration loosening resistance between $\beta = 0\%$ and $\beta = 50\%$. However, as shown in the figure, when β increased by more than 50%, κ clearly decreased. Specifically, in all cases, κ dropped rapidly from the start to $N \cong 50$ cycles (called initial loosening). The rate of decrease was approximately 7% or less for the DTB-IIC50, whereas it was approximately 15% for both the DTB-IIC60 and DTB-IIC70. After this initial loosening, κ for the DTB-IIC50 gradually decreased until $N \cong 200$ cycles, and then remained constant; its final value was more than 90%, which meets the rating-1 specified in ISO 16130, indicating good self-locking behavior. In contrast, κ for both the DTB-IIC60 and DTB-IIC70 gradually decreased until $N \cong 1000$, and then continued to decrease very slowly until the test end. As a result, the final values of κ for the DTB-IIC60 and DTB-IIC70 varied widely, decreasing by 70–75% and 60–65%, respectively, which corresponds to rating-2 in the ISO standard, meaning acceptable loss of clamping force. These results are assumed to be due to the contacting condition between the multi-thread grooves of the bolt and the threads of the inner nut as shown in Figs. 8(*a*)–8(*c*) and show that β has almost no effect on the vibration loosening resistance of DTB-IIC up to 50%, but clearly decreases the resistance beyond that value.

4 Conclusions

The following main outcomes were obtained from thread rolling simulations and experiments, and performance evaluation tests for DTB-IICs with different β values.

- The rolling formability of the DTB-IIC was much improved by increasing the bottom rise rate β for the multi-thread groove by 60–70%, and the problems of material peeling on the thread surface and high temperature produced by thread rolling, which remained issues in the previous study, were completely resolved.
- There was a clear difference in the rolling formability of the DTB-IIC due to the difference in processing methods, and the flat die and planetary methods more easily suppressed the occurrence of material peeling and improved the rolled thread surface finish compared to the conventional round die method. Comprehensive evaluation showed that the flat die type thread forming method was the best.
- The tensile strength for the DTB-IIC was hardly affected by higher β values, and its strength level exceeded the minimum tensile strength of SAE J429 strength grade 8.
- The results of the Junker vibration loosening test indicated that with the DTB-IIC50, the residual rate of the axial force after 2000 load cycles was more than 90%, which corresponds to rating-1 in the ISO standard. The vibration loosening resistance of the DTB-IIC clearly decreased when β increased by more than 50% because of a significant decrease in the contact area between the multi-thread nut and the screw threads. However, even with the DTB-IIC60 and DTB-IIC70, the axial force residual rate (70–75% and 60–65%, respectively) satisfied rating-2 in the ISO standard.

Conflict of Interest

There are no conflicts of interest.

Data Availability Statement

The authors attest that all data for this study are included in the paper.

Nomenclature

f = oscillation frequency in a Junker test
A = transverse displacement amplitude of the glider plate in a Junker test
N = total number of oscillations in a Junker test
F_M = initial axial preload of the bolt in a Junker test
α = amount of bottom rise of the multi-thread groove
β = bottom rise rate for the multi-thread groove
δ = amount of die radial feed
δ_{max} = final amount of die radial feed
ε = amount of deviation of the tips of the left and right parallelogram protrusions
η = die radial feed rate
κ = residual rate of axial load
ξ = thread cross-sectional area ratio

References

[1] Fukuoka, T., 2013, *Threaded Fasteners for Engineering and Design—Solid Mechanics and Numerical Analysis*, Corona Publishing Co., Ltd, Bunkyo-ku, Tokyo, pp. 263–321.

[2] Nishida, S., 1993, *Failure Analysis in Engineering Applications*, Butterworth Heineman Co., Ltd, Oxford, UK, pp. 68–104.

[3] Hongo, K., 1964, "Loosening of Bolt and Nut Fastenings," Trans. JSME Ser. I, **30**(215), pp. 934–939.

[4] Koga, K., 1969, "Loosening by Repeated Impact of Threaded Fastenings," Trans. JSME Ser. III, **35**(273), pp. 1104–1111.

[5] Yamamoto, A., and Kasei, 1977, "Investigation on the Self-loosening of Threaded Fasteners Under Transverse Vibration—A Solution for Self-loosening Mechanism," J. JSPE, **43**(508), pp. 470–475.

[6] Jingu, T., 1995, "Relationship Between Loosening Response of Bolt-Nut Fastening System and Stress Wave Modes Along the Direction of Propagation," Trans. JSME Ser. A, **61**(586), pp. 1398–1403.

[7] Izumi, S., Yokoyama, T., Kimura, M., and Sakai, S., 2009, "Loosening-Resistance Evaluation Double-Nut Tightening Method and Spring Washer by Three-Dimensional Finite Element Analysis," Eng. Fail. Anal., **16**(5), pp. 1510–1519.

[8] Miyata, C., 1985, "Proposal of Loosening-Proof Nuts (Stress Distribution in a Bolted Joint and Pressure Distribution on Bearing Surface of Nut)," Trans. JSME Ser. C, **51**(467), pp. 1833–1837.

[9] Sase, N., Nishioka, K., Koga, S., and Fujii, H., 1998, "An Anti-loosening Screw-Fastener Innovation and Its Evaluation," J. Mater. Process. Technol., **77**(1–3), pp. 209–215.

[10] Noda, N., Wang, B., Sano, Y., Kawano, R., Liu, X., Inui, Y., and Takase, Y., 2022, "Investigation of Loosening Resistance Based on Junker Loosening Test of Bolt Nut Connections With Pitch Difference," JSAE Trans., **53**(2), pp. 410–417.

[11] Kase, S., 1985, "On the Self-loosening Mechanism of Bolted Joints Under Transverse External Force," J. JSPE, **51**(9), pp. 1783–1788.

[12] Ohashi, N., and Ishimura, M., 1985, "On Thread-Loosening Test by Transversely Repeated Impact Force," J. JSPE, **51**(6), pp. 1264–1268.

[13] Kase, S., Ishimura, M., and Ohashi, N., 1988, "On Self-loosening of Threaded Joints in the Case of Absence of Macroscopic Bearing-Surface Sliding-Loosening Mechanism Under Transversely Repeated Force," J. JSPE, **54**(7), pp. 1381–1386.

[14] Ishimura, M., Yamanaka, H., Syoji, Y., Kobayashi, T., and Sawa, T., 2011, "Loosening of Bolted Joints Under Transverse Repeated Displacement," Trans. JSME Ser. A, **77**(781), pp. 1444–1452.

[15] Nagawa, M., Saito, K., and Noda, N., 2003, "Study on Anti-loosening Super Lock Nuts and Super Lock Bolts (First Volume)," Mach. Des., **47**(8), pp. 35–42.

[16] Takemasu, T., and Miyahara, H., 2005, "Development of Thread Rolled Anti-loosening Bolts Based on the Double Thread Mechanism and a Performance Evaluation," JSME Int. J. Ser. A, **48**(4), pp. 305–310.

[17] Karlsena, Ø., and Lemua, H. G., 2022, "Comparative Study on Loosening of Anti-loosening Bolt and Standard Bolt System," Eng. Fail. Anal., **140**, 106590.

[18] Shinbutsu, T., Amano, S., Takemasu, T., and Kuwabara, T., 2017, "Thread Rolling and Performance Evaluation of New Double-Thread Bolt—Study on Development of Antiloosening Bolt Fasteners Based on Coarse-Single Coarse-Multiple Double-Thread Mechanism, 1st Report," J. JSTP, **58**(676), pp. 404–410.

[19] Shinbutsu, T., Amano, S., Takemasu, T., Kuwabara, T., and Shimura, J., 2017, "Thread Rolling and Performance Evaluation of a New Anti-loosening Double Thread Bolt Combining a Single Thread and Multiple Threads," Procedia Eng., **207**, pp. 603–608.

[20] Shinbutsu, T., Amano, S., Takemasu, T., Shimura, J., Sakamoto, M., and Kuwabara, T., 2018, "Thread Rolling and Performance Evaluation of Modified Double-Thread Bolt—Study on Development of Antiloosening Bolt Fasteners Based on Coarse-Single Coarse-Multiple Double-Thread Mechanism, 2nd Report," J. JSTP, **59**(688), pp. 71–77.

[21] Amano, S., Shinbutsu, T., Okimoto, Y., Takemasu, T., and Kuwabara, T., 2024, "Optimization of Anti-loosening Bolt Based on Double Thread Mechanism: Development of Ground Rolling Die and Effect of Thread Accuracy on Loosening Resistance," Heliyon, **10**(2024), p. e28631.

[22] Junker, G. H., 1969, "New Criteria for Self-loosening of Fasteners Under Vibration," SAE Trans., **78**, pp. 314–335.

[23] Pichoff, F., Kummel, M., and Schiff, M., 2018, "Dynamic Vibration Testing of Fasteners: Fastener Self-loosening Theory, Vibration Testing Practical Applications, Comparison of the International Standards and Recommendations on How to Set-up a Meaningful Testing Protocol," Mater. Tech., **106**(3), p. 307.